GNSS-assisted accurate corridor mapping with small UAV

Y. Zhou, E Rupnik, P-H Faure, M. Pierrot-Deseilligny

GNSS-assisted accurate corridor mapping with small UAV

Y. Zhou[1] E. Rupnik[1] P-H. Faure[2] M.Pierrot-Deseilligny[1]

[1] IGN-ENSG, Institut National de l'Information Géographique et Forestière
[2] C.N.R - CACOH, Compagnie Nationale du Rhône

Yilin.Zhou@ensg.eu

Résumé

Avec le développement des véhicules aériens sans pilote (UAV) et du système de positionnement par satellites (GNSS), les positions précises de la caméra à l'exposition peuvent être connues et l'approche ajustement de faisceau (BBA) assisté par GNSS est devenu possible pour l'orientation des images. L'estimation de multiples bras de levier dans la procédure BBA permet de fusionner des blocs d'images de différentes configurations telle que des images nadir et obliqueset ainsi obtenir une meilleure précision. En raison du coût substantiel de l'établissement d'un réseau de points d'appui (GCP), un nombre minimal de GCPs est attendu tout en maintenant la précision. En ajoutant un bloc d'images oblique au bloc d'images nadir ou en fusionnant des blocs d'images nadir de différentes hauteurs de vol, une précision de ~ 5 cm *est atteinte sans GCP sur une scène d'acquisition corridor de* ~ 600 m. *Cette précision est également obtenue avec uniquement un bloc d'images nadir en fournissant une bonne calibration a priori de la caméra . Avec un GCP au milieu du bloc d'images, la précision verticale est significativement améliorée et une précision de* ~ 1.0 cm *est atteinte.*

Mots Clef

précision, automatisation, UAV, GNSS, point d'appui au sol.

Abstract

With the development of unmanned aerial vehicles (UAVs) and global navigation satellite system (GNSS), the accurate camera positions at exposure can be known and the GNSS-assisted bundle block adjustment (BBA) approach is possible for image orientation. Several flights are conducted on a dike with a small UAV embedded with a metric camera and GNSS receiver. The multi-lever-arm estimation within the BBA procedure makes it possible to merge image blocks of different configurations such as nadir and oblique images and thus achieve a better accuracy. Due to the substantial cost of ground control point (GCP) network establishment, a minimum number of GCPs is expected while maintaining the 3D point accuracy. By adding oblique image block to nadir image block or merging nadir image blocks of different flight heights, a 3D point accuracy of ~ 5 cm *is reached with no GCPs on a corridor acquisition scene of* ~ 600 m. *This 3D point accuracy is as well achieved with solely a nadir image block by providing a good a priori camera calibration. With one GCP in the middle of the image block, the vertical accuracy is significantly improved and a 3D point accuracy of* ~ 1.0 cm *is attained.*

Keywords

accuracy, automation, UAV, GNSS, ground control point

1 Introduction

For traditional airborne photogrammetry with unmanned aerial vehicles (UAVs), the exterior orientation (EO) parameters are determined indirectly using the well-known method bundle block adjustment (BBA). The BBA method is effective and widely employed for photogrammetric production when the scene is well-textured and allows for automated tie point extraction.

3D point accuracy are strongly dependent on the geometry of acquisition field and the number of ground control points (GCPs) as well as their distribution within the image block [12, 20]. Among different configurations of UAV acquisitions, the corridor mapping has a high potential in such as dike surveillance, highway planning and power line surveys. Nevertheless, it can also be challenging in many aspects. With the special geometry, a well-distributed GCP network is not easy to ensure. The acquired images are often in strips, which makes it difficult to have satisfying sidelaps and thus results in less accurate EO parameter determination. While the employment of a large number of GCPs prevents model distortion, the field work of ground control point establishment can be substantially expensive and time-consuming.

With the appearence and development of global navigation satellite system (GNSS), it is possible to know the accurate camera perspective center positions at exposure and thus to eliminate the requirement of GCPs within the image block [11, 15]. However, several GCPs are still used for

the purpose of improving the redundancy and identifying possible bias in GNSS positioning [1, 6]. When coupling this GNSS-assisted bundle block adjustment approach to an inertial navigation system (INS), the EO parameters can be determined directly for each image without auxiliary information coming from the traditional AT procedure. For small UAVs, an accurate position and attitude aerial control remains challenging due to the limited availability of weight, power and volumn in the UAV payload.

Different researches have been carried out to mitigate errors in INS/GNSS system. The linear offset lever-arm can be determined indirectly by computing the difference between GNSS-derived positions of antenna reference point and camera perspective centers resulting from bundle block adjustment [4]. This offset can also be estimated as an additional parameter during the bundle block adjustment whereas the accuracy is limited due to its correlation with camera interior orientation parameters [17, 8]. While with classical methods (by a calliper or by photogrammetric approaches) the linear offset lever-arm can be determined, it is not possible for the boresight calibration to reach sufficient accuracy in the same way. Several boresight calibration methods have been proposed [14, 7, 2, 10]. It can be performed either with "one-step" method (estimation within self-calibration process) or with "two-step" method (comparison of the INS/GNSS-derived attitude with that obtained by AT procedure). Moreover, taking into account the remaining temporal correlations within the navigation system can lead to a more realistic estimation [16]. Despite the possibilities of improving the INS/GNSS system accuracy, the INS system demands more effort to reduce errors and often needs accurate GNSS positions as constraints for error control. This demand on precision and thus on high quality of INS/GNSS sensors can be complicated given the limited UAV payload capability.

Therefore, for small UAV photogrammetric acquisitions, the assisted bundle block adjustment with GNSS data and GCPs seems to be a more interesting approach. Given the substantial inconvenience and cost of GCP establishment especially in areas with difficult access, the number of GCPs is needed to be reduced to a strict minimum.

The research results of V. Tournadre [18] showed that for corridor mapping performed with small UAVs, by optimising the camera model and combining nadir and oblique images, a centimetric accuracy is attained with one GCP every 100 m. With embedded GNSS module on small UAVs, the GNSS-derived camera positions at exposure is used for integrated sensor orientation (ISO) of camera pose [3]. An accuracy of a few centimeters is reached with one single GCP.

1.1 Problem Formulation

With the development and increasing employment of UAVs in photogrammetric production as well as the possibility of knowing accurate camera perspective center positions with the aid of GNSS system, the need of well-distributed GCP network within the image block can be eliminated and only a few GCPs are required to improve the redundancy and to identify possible bias in GNSS positionning. Given the special geometry, corridor mapping has a higher demand on the quality of GCP network whilst the establishment can be expensive and time-consuming. In this paper, a UAV acquisition of a dike is presented and the accuracy of this corridor configuration that can be obtained with a small number of GCPs is investigated.

1.2 Paper Structure

The following part of this article gives brief introduction of the employed UAV system and sensors. In section 3 the nature of the acquisition field is described and the information of conducted flights are presented. The following section is devoted to the data processing pipeline with the focus on the integration of GNSS data and its improvement on tie point extraction efficiency. Finally, the results of conducted acquisitions are presented and the mapping accuracy is evaluated. Conclusions are drawn in the last section, as well as recommendations for further investigations.

2 System Design

2.1 UAV

The chosen UAV is a Copter 1B of SURVEY Copter which is robust and reliable. It has a wingspan of 1.82 m and a length of 1.66 m. Powered by a gasoline engine, the maximal payload capacity of the UAV is 4.1 kg and the endurance is up to 60 min.

2.2 Camera

The chosen camera for data acquisition, a home-made metric camera CamLight, is designed specifically to meet the needs of photogrammetric UAV acquisitions by laboratory LOEMI [1] of IGN [2][9]. The compact camera body without lens has a low mass of 160 g and is compatible with most commercially available lenses. Within the acquisition, the camera is equipped with a full frame sensor of 5120×3840 pixels and a 35 mm lens (140 g). The camera is triggered with an intervalometer every 2.5 s and powered by the onboard power system.

2.3 GNSS Receiver

The chosen GNSS receiver is a GPS monofrequency receiver with L1 GPS antenna and is integrated to the camera system. The GPS time of exposures is provided by the GPS module and is registered in the header file for

1. Laboratoire d'Opto-éléctrique et de Métrologie et d'Instrumentation
2. Institut National de l'Information Géographique et Forestière

each image. Within the acquisition, the GPS module works at 1Hz frequency.

The aforementioned hardwares are presented in Figure 1.

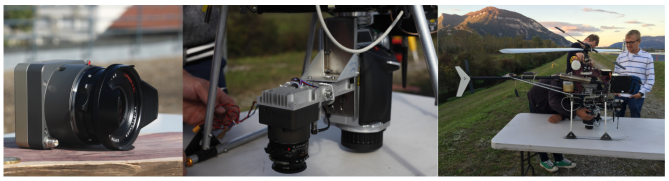

FIGURE 1 – CamLight (left), camera set-up on UAV (middle), UAV (right)

3 Data Acquisition

3.1 Acquisition Field

On October 4, 2017, several flights are conducted in Culoz, France. The acquisition field is a north-south orientated dike of $\sim 1.2\mathrm{km}$ long with a turn on the north end. The scene has a corridor configuration with little height difference, which is challenging for photogrammetric UAV acquisitions. 41 points were regularly placed along the acquisition field and surveyed to be used either as ground control points (GCP) or check points (CP).

3.2 Flight Design

According to the flight autorization issued by the DGAC [3], the distance between the telepilot and the UAV employed for the acquisition can not surpass 600 m. Therefore, the acquisition field is divided into 2 segments of 600 m and surveyed separately. The first segment of 600 m consists of the south part of the dike while the second segment consists of the rest of the dike including the turn on the north end. Figure 2 depicts the conducted flights and the information of flights are given in Table 1.

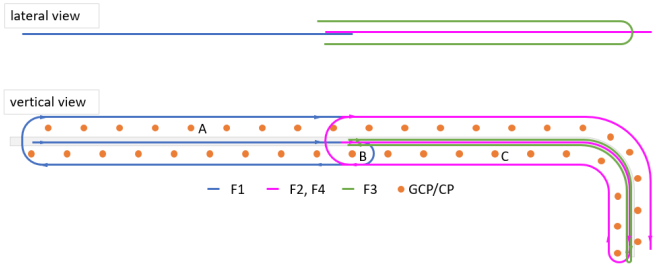

FIGURE 2 – An illustration of executed flights

The segment 1 (S1) is surveyed with one nadir flight of 3 strips at 50 m (F1) while the segment 2 (S2) consists of 3 flights (F2-F4). F2 (nadir) and F4 (oblique) share the same configuration with F1. F3 is a nadir flight of 2 single strip at different heights (30 m and 70 m) to better de-correlate IO/EO parameters.

3. Direction Générale de l'Aviation Civil

Segment		S1	S2		
Flight		F1	F2	F3	F4
Nb of images		395	315	200	323
Height (m)		50	50	30, 70	50
Orientation		nadir			oblique
Nb of strips		3	3	1	3
Overlap (%)	forward	80			
	side	70			
GCP accuracy (mm)	horizontal	1.3			
	vertical	1			
GSD (m)		0.1			

TABLE 1 – Information of flights

4 Data Processing

The photogrammetric data processing is performed with MicMac, a free open-source photogrammetric software developped at IGN and ENSG [4] since 2003 [13].

4.1 Synchronization of GNSS and Camera System

The GNSS data is post-processed using RTKLib in carrier-phase differential mode with respect to a base station installed on the south end of the dike. The position of this base station is precisely determined by processing a $\sim$ 24 hour static observation session over two days with the service provided by IGN. With a sampling frequency of 1 Hz, one position is calculated every second. Nevertheless, the frequency of image acquisition is of 0.4 Hz, which introduces a desynchronization between GNSS and camera system. So as to determine the position of the camera at exposure, a parabolic interpolation is carried out taking into account the GNSS-derived position accuracy and velocity. Figure 3 depicts the desynchronization between the two systems; circles in blue represent GNSS-derived positions and pyramids represent camera frames.

FIGURE 3 – An illustration of the desynchronization between GNSS (blue circles) and camera (pyramid) system

4.2 Processing Methodology

In order to render the tie point extraction more efficient, a list of overlapped image couples is generated with the benefit of known camera positions at exposure. Tie point extraction is then performed on listed image couples. However, without the ackonwledgement of image attitudes, the determination of overlapped image couples is based solely on image positions thus not complete. Image attitude information is provided by performing relative bundle block adjustment on images with currently existed tie points as input and the list of overlapped image couples

4. Ecole Nationale des Sciences Géographiques

is then completed. A second iteration of tie point extraction is performed on newly added overlapped image couples.

For an image block of 395 images acquired with flight F1, the tie point extraction will be performed on 77815 image couples if no a priori information of camera positions is given, the computation procedure takes ~ 5 h. While with the above-mentioned two iterations of tie point extraction, the computation only took 2h15min.

The IO/EO parameters in a relative scale are determined with a hybrid internal model coupling a high degree correction of radial distortion (up to R^{15}) and a general polynomial one for empirical distortion correction. Camera positions are then employed for transformation into an absolute scale. An absolute bundle block adjustment is performed with tie points, GNSS-derived camera positions and GCPs as observations.

The mathematical model of the performed absolute bundle block adjustment is presented as follows. The objectif is to minimize a global energy function :

$$\mathcal{E} = \sum_{l=1}^{L}\sum_{m=1}^{M} \frac{(p_{l,m} - \zeta(\pi(R_m(P_l - C_m))))^2}{\sigma_{im}^A} \quad (1)$$

$$+ \sum_{z=1}^{Z}\sum_{k=1}^{K} \frac{(R_k(C_k - C_{\text{gnss},k}) - \vec{\theta}_z)^2}{\sigma_{gnss}} \quad (2)$$

$$+ \sum_{n=1}^{N} \frac{(P_n - P_{\text{gcp},n})^2}{\sigma_{gcp}} \quad (3)$$

$$+ \sum_{n=1}^{N}\sum_{m=1}^{M} \frac{(p_{n,m} - \zeta(\pi(R_m(P_{\text{gcp},n} - C_m))))^2}{\sigma_{im}^H} \quad (4)$$

where : l is the index of tie points ;
m is the index of images ;
z is the index of image blocks defined by lever-arm ;
k is the index of images with GNSS measurements ;
n is the index of GCPs ;
ζ is the camera model ;
π is the projection function ;
$p_{l,m}$ is the 2D position of tie point l in image m ;
(R_m, C_m) is the pose of image m ;
P_l is the 3D position of tie point l ;
C_k is the camera perspective center of image k ;
$C_{\text{gnss},k}$ is the phase center of GNSS antenna of image k ;
R_k is the world to camera rotation ;
$\vec{\theta}_z$ is the lever-arm of image block z ;
P_n is the pseudo-intersection position of GCP n ;
$P_{\text{gcp},n}$ is the ground measurement of GCP n ;
$p_{n,m}$ is the image measurement of GCP n in image m ;
σ_{im}^A is the weight of tie points in images ;
σ_{gnss} is the weight of GNSS measurements ;
σ_{gcp} is the weight of GCPs ;
σ_{im}^H is the weight of image measurements of GCPs ;

The global energy function is composed of 4 parts : (1) the energy of tie points, (2) the energy of GNSS measurements, (3) the energy of GCPs and (4) the energy of image measurements of GCPs. The minimization problem is solved with Levenberg-Marquardt (L-M) method. The L-M is in essence the Gauss-Newton method enriched with a damping factor to handle rank-deficient Jacobian matrices [21].

Within the procedure, the lever-arm for each image block is determined as an additional parameter of the model. When flights of different configurations are merged and processed, one lever-arm per image block is estimated. This makes it possible to merge image block datasets acquired on the same acquisition field while having different configuration (e.g., nadir and oblique images, etc...)

The accuracy is evaluated with CPs and the root-mean-square (RMS) of check point residuals is used as the accuracy criteria. Figure 4 depicts the aforementioned data processing pipeline.

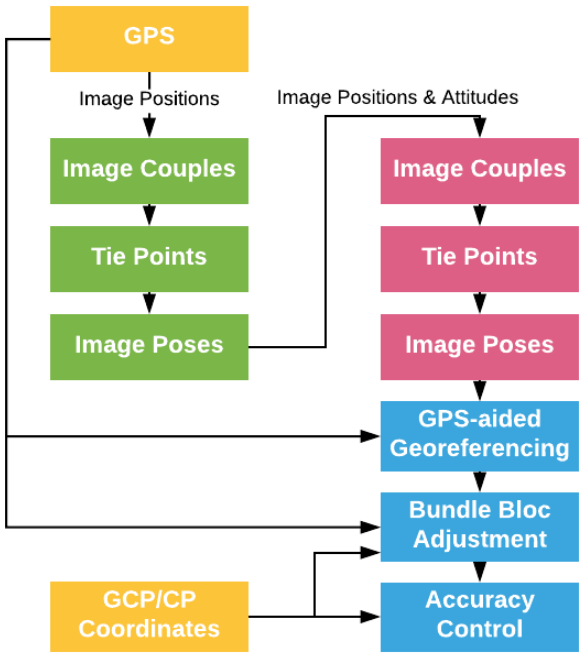

FIGURE 4 – Data processing pipeline

5 Results

5.1 Combination of Flights

Several combinations of flights are investigated to benefit the presence of different configurations. The information of different flight combinations is given in Table 2.
With the combination C1, a better sidelap and a greater angle of perspective ray intersections are provided with the existence of oblique images, which is recommanded

	Segment	Flight
C1	S2	F2 + F4
C2		F2 + F3 + F4
C3	S1	F1
C4	S1 + S2	F1 + F2 + F3 + F4

TABLE 2 – Information of flight combinations

for acquisition scenes of little height difference [5, 19]. By comparing the obtained accuracy of combination C1 and C2, the impact of including images of different heights is investigated. For combination C3 with only nadir images, the results with and without a priori camera calibration are compared. Combination C4 gives an indication of how accuracy varies when the length of acquisition field changes and the achievable accuracy with a few GCPs. Results for each flight combination is given in Table 3.

	Comb	GCP	GNSS	RMS (cm)		
				horizontal	vertical	3D
V1	C1	0	F2 + F4	1.7	8.5	8.7
V2		1		0.6	0.7	0.9
V3	C2	0		2.0	4.5	4.9
V4		1		0.8	0.9	1.2
V5	C3	0	F1	1.6	20.2	20.3
V6		1		1.4	1.5	2.0
V7		0		1.3	4.8	5.0
V8		1		1.2	0.7	1.4
V9	C4	0	F1 + F2+F4	1.4	5.4	5.5
V10		1		1.4	1.4	2.0
V11		2		1.0	0.7	1.2

TABLE 3 – Residuals on check points

For C1 and C2, the only GCP used is point C as shown in Figure 2 and the rest are used as CPs to evaluate the accuracy. For C1, the bundle block adjustment is performed with tie points, GNSS-derived camera positions (with and without point C as GCP) as input. For C2, a bias on vertical component is observed on GNSS-derived camera positions for F3 and a proper estimation of the lever-arm for this flight is not feasible. Therefore these GNSS-derived camera positions are eliminated from the following bundle block adjustment. The differences on accuracy between V1-V2 and V3-V4 show that, with only tie points and GNSS-derived camera positions the model is less accurate on vertical component than on horizontal one. This is mainly due to the small height difference on acquisition scene. Adding at least one GCP will improve the accuracy especially on vertical component. By investigating the difference on accuracy between V1-V3, an improvement is observed on vertical component after including tie points from flights of different heights. It can be explained by the fact that the IO/EO parameters are better de-correlated. However, the difference of accuracy between V2-V4 shows that the accuracy declines slightly by only adding tie points of different flight heights without adding the corresponding GNSS-derived camera positions. The newly added images are not perfectly oriented under the constraints of tie points and one GCP, which also reflects the impact of GNSS-derived camera positions on 3D point accuracy.

Point A is used as GCP for C3 dataset. V5 and V6 are processed without the self-calibration step, i.e., IO parameters are not determined a priori. V7 and V8 are processed with the IO parameters coming from V2 and the IO parameters are fixed during the determination of EO parameters. In the configuration of V5 only tie points of nadir images and GNSS-derived camera positions are used for bundle block adjustment and no a priori camera calibration is provided, the addition of oblique images (V1) does not have great impact on horizontal accuracy whereas improves considerably the vertical accuracy since the inclusion of oblique images enhanced the sidelap and increased the intersection angle between perspective rays. The inclusion of point A as GCP (V6) in the bundle block adjustment renders better determination of the focal length and then a better vertical accuracy compared to V5. The difference between V5 and V7 indicates the importance of a good camera calibration.

For C4, point B is used when one GPS is included in bundle block adjustment whilst point A and C are used for two GCPs configuration. The camera calibration of V2 is provided and fixed during the bundle block adjustment. For a corridor configuration of $\sim$ 1200 m, a 3D point accuracy of $2\mathrm{cm}$ is reached with one GCP by performing the GNSS-assisted bundle block adjustment.

6 Conclusion

The GNSS-assisted bundle block adjustment makes it possible to eliminate the requirement of GCPs for EO parameter determination. The use of a few GCPs improves the redundency and identifies possible bias in GNSS positionning. Due to the substential cost of field work, the number of GCPs is expected to be a minimum while maintaining the accuracy.

Several flights are conducted on a dike of $\sim$ 1200 m of which the corridor geometry and the little height difference remain challenging for photogrammetric acquisitions. By investigating results of different image block configurations, the following conclusions are drawn.

When performing the GNSS-assisted bundle block adjsment without GCPs to a nadir image block, the vertical accuracy is not ensured mainly due to the little height difference of the acquisition field. The inclusion of oblique images enhanced the sidelap and increased the intersection angle between perspective rays. The addition of images of different height flights rendered a better de-correlation of

IO/EO parameters. Both these two strategies mitigated the vertical inaccuracy and the 3D point accuracy is ~ 5.0 cm. Given a good camera calibration, the 3D point accuracy of ~ 5.0 cm is achieved with solely nadir images. To further improve the accuracy (especially on vertical component), one GCP located in the center of the image block is used and the 3D point accuracy reached ~ 1.0 cm. For the corridor acquisition scene of ~ 1200 m, the 3D point accuracy is 2 cm with one GCP in the middle and 1.2 cm with 2 GCPs.

Because of the observed bias on vertical component for F3, the GNSS-derived camera perspective positions are not exploited during the bundle block adjustment procedure. In further studies, the impact when adding images of different flight heights and corresponding GNSS measurements should be investigated thoroughly.

Références

[1] Fritz Ackermann. Operational rules and accuracy models for gps-aerotriangulation. *Arch. ISPRS*, 1 :691–700, 1992.

[2] M Cramer and D Stallmann. System calibration for direct georeferencing. *International Archives of Photogrammetry Remote Sensing and Spatial Information Sciences*, 34(3/A) :79–84, 2002.

[3] M Daakir, Marc Pierrot-Deseilligny, Pierre Bosser, Francis Pichard, Christian Thom, Yohann Rabot, and Olivier Martin. Lightweight uav with on-board photogrammetry and single-frequency gps positioning for metrology applications. *ISPRS Journal of Photogrammetry and Remote Sensing*, 127 :115–126, 2017.

[4] Cameron Ellum and NASER EL-SHEIMY. Inexpensive kinematic attitude determination from mems-based accelerometers and gps-derived accelerations. *Navigation*, 49(3) :117–126, 2002.

[5] CLIVES FRASER. Limiting error propagation in network design((in photogrammetry)). *Photogrammetric Engineering and Remote Sensing*, 53 :487–493, 1987.

[6] Christian Heipke, Karsten Jacobsen, and Helge Wegmann. *Integrated sensor orientation : Test report and workshop proceedings*. Bundesamt für Kartographie und Geodäsie, 2002.

[7] Erwin Kruck. Combined imu and sensor calibration with bingo-f. In *Integrated Sensor Orientation, Proc. of the OEEPE Workshop". Hannover : CD-ROM*, 2001.

[8] Derek Lichti, Jan Skaloud, and Philipp Schaer. On the calibration strategy of medium format cameras for direct georeferencing. In *International Calibration and Orientation Workshop EuroCOW*, number TOPO-PRESENTATION-2008-001, 2008. all-airborn approach, self-calibration, parameter correlation, field depth constraints focal length estimation.

[9] Olivier Martin, Christophe Meynard, Marc Pierrot Deseilligny, Jean-Philippe Souchon, and Christian Thom. Réalisation d'une caméra photogrammétrique ultralégère et de haute résolution. In *Proceedings of the colloque drones et moyens légers aéroportés d'observation, Montpellier, France*, pages 24–26, 2014.

[10] MR Mostafa. Camera/imu boresight calibration : New advances and performance analysis. In *Proceedings, ASPRS Annual Meeting, Washington, DC, April*, pages 21–26, 2002.

[11] Martin Rehak and Jan Skaloud. Fixed-wing micro aerial vehicle for accurate corridor mapping. *ISPRS Annals of the Photogrammetry, Remote Sensing and Spatial Information Sciences*, 2(1) :23, 2015.

[12] Fabio Remondino, L Barazzetti, Francesco Nex, Marco Scaioni, and Daniele Sarazzi. Uav photogrammetry for mapping and 3d modeling–current status and future perspectives. *International Archives of the Photogrammetry, Remote Sensing and Spatial Information Sciences*, 38(1) :C22, 2011.

[13] Ewelina Rupnik, Mehdi Daakir, and Marc Pierrot Deseilligny. Micmac–a free, open-source solution for photogrammetry. *Open Geospatial Data, Software and Standards*, 2(1) :14, 2017. MicMac history, organisation and features.

[14] J Skaloud, M Cramer, and KP Schwarz. Exterior orientation by direct measurement of camera position and attitude. *International Archives of Photogrammetry and Remote Sensing*, 31(B3) :125–130, 1996.

[15] Jan Skaloud, Martin Rehak, and Derek Lichti. Mapping with mav : Experimental study on the contribution of absolute and relative aerial position control. *The International Archives of Photogrammetry, Remote Sensing and Spatial Information Sciences*, 40(3) :123, 2014.

[16] Jan Skaloud and Philipp Schaer. Towards a more rigorous boresight determination : Theory, technology and realities of inertial/gps sensor orientation. In *Proceedings of the ISPRS, WG 1/5 Platform and Sensor Integration Conference*, number TOPO-CONF-2005-006, 2003.

[17] Jan Skaloud and Julien Vallet. High accuracy handheld mapping system for fast helicopter deployment. *INTERNATIONAL ARCHIVES OF PHOTOGRAMMETRY REMOTE SENSING AND SPATIAL INFORMATION SCIENCES*, 34(4) :614–619, 2002.

[18] Vincent Tournadre. *Métrologie par photogrammétrie aéroportée légère : application au suivi d'évolution de digues*. PhD thesis, Université Paris-Est, 2015.

[19] Bill Triggs. Autocalibration from planar scenes. In *European Conference on Computer Vision*, pages 89–105. Springer, 1998.

[20] Julien Vallet, Flory Panissod, Christoph Strecha, and M Tracol. Photogrammetric performance of an ultra light weight swinglet uav. In *UAV-g*, number EPFL-CONF-169252, 2011.

[21] Stephen Wright and Jorge Nocedal. Numerical optimization. *Springer Science*, 35(67-68) :7, 1999.